國立交通大學

物理研究所

碩 士 論 文

GZK 邊界與極高能宇宙射線能譜

GZK horizons and ultra-high energy cosmic ray spectrum

研 究 生：盧佳均

指導教授：林貴林　教授

中 華 民 國 九十七 年 七 月

GZK 邊界與極高能宇宙射線能譜

GZK horizons and ultra-high energy cosmic ray spectrum

研 究 生：盧佳均　　Student：Chia-Chun Lu

指導教授：林貴林　　Advisor：Guey-Lin Lin

國 立 交 通 大 學

物理研究所

碩 士 論 文

A Thesis

Submitted to Institute of Physics

College of Science

National Chiao Tung University

in Partial Fulfillment of the Requirements

for the Degree of

Master

in

Physics

July 2008

Hsinchu, Taiwan, Republic of China

中華民國九十七年七月

GZK 邊界與極高能宇宙射線能譜

學生：盧佳均　　指導教授：林貴林

國立交通大學物理研究所碩士班

摘　　要

本論文中，我們研究極高能宇宙射線源分佈及對於 GZK 邊界的影響，此研究動機來自 Pierre Auger 最近所發表的極高能宇宙射線與鄰近活躍星系核之關聯性研究。我們利用極高能宇宙射線能譜計算其對於鄰近區域宇宙射線源分佈的限制，這會影響 GZK 邊界的估計。同時我們在研究中引進可能的能量校正，我們認為鄰近地區宇宙射線源的密度可能大於平均密度，而這可以在未來觀測數據更多的時候得到檢驗。

GZK horizons and ultra-high energy cosmic ray spectrum

Student：Chia-Chun Lu　　Advisor：Dr. Guey-Lin Lin

Institute of **Physics**
National Chiao Tung University

ABSTRACT

Motivated by recent Pierre Auger result on the correlation of the highest-energy cosmic rays with the nearby active galactic nuclei, we explore possible ultrahigh energy cosmic ray (UHECR) source distributions and their effects on GZK horizons. Effects on GZK horizons by local over-density of UHECR sources are examined carefully with constraints on the degree of local over-density inferred from the measured UHECR spectrum. We include the energy calibration effect on the Pierre Auger data in our studies. We propose possible local over-densities of UHECR sources which are testable in the future cosmic ray astronomy.

誌　　謝

感謝我的父母親，懷著擔憂的心情，無怨無悔地一路支持我這個任性的女兒。感謝林貴林老師，對我的包容與鼓勵，讓我找回隱藏在我名字裡卻失落已久的〝自信〞與〝勇氣〞(Confidence-Courage)。感謝口試委員以及師長們：高文芳老師、張祥光老師、林及仁老師、黃明輝老師、王正祥老師，對於我研究及論文的建議與指導。感謝永順學長，宗哲學長，鳳吟學姊給我各方面尤其是電腦使用上的協助。感謝同學們的陪伴，讓我在交大這兩年的生活快樂而多采多姿。感謝我的小鬥，教了我一件最重要的事情。最後感謝上天，冥冥之中無形的力量，帶給我這些。無論未來的路是否平順，這兩年都是我會一生珍藏回憶的光輝歲月。

Contents

中文提要	……	i
Abstract	……	ii
誌謝	……	iii
Contents	……	iv
Table List	……	v
Figure List	……	vi
1.	**Introduction……**	**1**
1.1	Ultra high energy cosmic ray spectrum and detections……	2
1.2	Composition measurements……	4
1.3	Features of UHECR spectra……	5
1.3.1	GZK cutoff……	5
1.3.2	Energy calibration between different experiments……	7
1.4	Correlation sources search……	8
1.5	GZK horizon and inconsistency in Auger's analysis……	9
1.6	Solutions to the departure between GZK horizon and valid distance of V-C catalog……	11
1.6.1	Local over-density of UHECR sources……	11
1.6.2	Effects of energy calibration……	12
2.	**Research methods……**	**13**
2.1	Cosmic ray propagation and energy loss……	13
2.2	Source evolution models……	14
2.3	Spectrum fittings……	15
3.	**GZK horizons……**	**16**
3.1	The accumulative event probabilities of UHECR……	16
3.2	GZK horizons and local over-densities……	17
4.	**Fittings to the UHECR spectrum measured by Pierre Auger……**	**19**
4.1	Fittings to the unshifted spectrum……	19
4.2	Fittings to the shifted specturm……	20
5.	**Conclusions……**	**25**
Bibliography	……	**27**

Table List

3.1	GZK horizons of UHECR ……	18
4.1	χ^2 values from fittings to the Auger measured spectrum ……	20
4.2	χ^2 values from fittings to the shifted Auger spectrum ……	23
5.1	Percentages of cosmic ray events that come from sources within 30Mpc……	26

Figure List

1.1	The Cosmic ray spectrum……	2
1.2	The diagram of air shower development……	3
1.3	The fluorescence and surface detectors……	4
1.4	The sites of four recent UHECR observatories……	5
1.5	The X_{max}-energy diagram……	6
1.6	UHECR spectra from different measurement……	7
1.7	Attenuation lengths of cosmic ray energy loss processes……	8
1.8	Candidates for UHECR sources in Hillas plot……	9
1.9	Events and the correlated sources in Auger's search……	10
3.1	The accumulative event probability as a function of D……	17
4.1	Fittings to the Auger spectrum for γ =2.5 and 2.6……	21
4.2	Fittings to the Auger spectrum for γ =2.7……	22
4.3	Fittings to the shifted Auger spectrum for γ =2.4and 2.5……	23
4.4	Fittings to the shifted Auger spectrum for γ =2.6……	24

Chapter 1

Introduction

This thesis was motivated by the newest result of Pierre Auger Observatory on the correlation of the highest-energy cosmic rays with the nearby active galactic nuclei.[1, 2]. Here we examined the consistency in their analysis. The present understanding on ultra-high energy cosmic ray is described in Section 1.1, 1.2 and 1.3. Auger's result is presented in Section 1.4 and questions aroused from this result are stated in Section 1.5. In Section 1.6, we offer possible solutions.

The details of our research method are presented in Chapter 2. We discuss about GZK horizons in Chapter 3. We calculate accumulated event probabilities of UHECR for arrival threshold energies at 57, 70, 80 and 90 EeV respectively. GZK horizons corresponding to different threshold energies are tabulated. We also calculate a similar set of GZK horizons with local over-density of UHECR sources taken into account. In Chapter 4, we perform fittings to the measured UHECR spectrum, which includes the effect from the local over-density of UHECR sources. The constraint on the degree of local over-density is presented. To study effects of energy calibrations, we also perform fittings to the energy-adjusted UHECR spectrum with local over-density of UHECR sources considered. We compare results from both fittings. Chapter 5 is the conclusion.

1.1 Ultra high energy cosmic ray spectrum and detections

The systematic study of Ultra High Energy Cosmic Rays (UHECR) started in late 1950s after construction of Volcano Ranch (USA) and Moscow University (USSR) arrays. The first ultra high energy cosmic ray (UHECR) with an energy about 10^{20} eV was detected by Volcano Ranch array in 1962. During the next few decades of research, the origin of UHECR was not well understood. At present, data from Yakutsk (Russia) [3], AGASA (Japan)[4, 5] , HiRes (USA)[6] and Pierre Auger (International collabration)[7] offer some hints of this long-standing mystery.

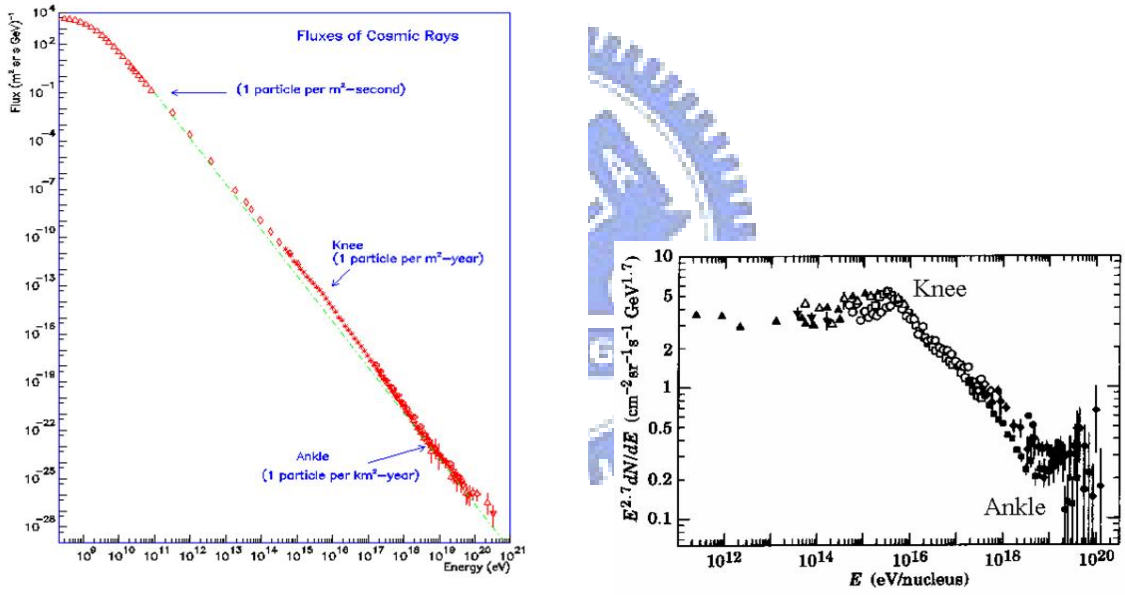

Figure 1.1: The left panel presents the cosmic ray spectrum which expands 12 decades of energies. It is assembled by several measurements. This figure is reproduced by Angela V. Olinto[8]. The right panel enlarges the highest energy region. After multiplied by $E^{2.7}$ on the flux, the spectrum turn into an impressive shape like a leg with a knee and an ankle at energy $10^{15.5}$ and $10^{18.5}$ eV respectively.

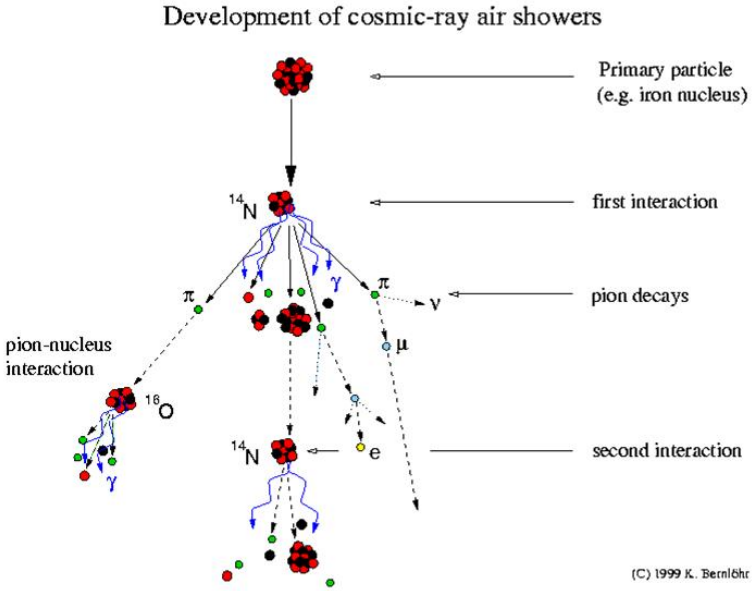

Figure 1.2: The diagram of air shower development.

Figure 1.1 shows the entire cosmic ray spectrum which expands over 12 decades of energies. There are two transition points named the knee and the ankle at energy $10^{15.5}$ and $10^{18.5}$ eV respectively. At the highest energy region above 10^{19} eV, the flux is as low as 1 particle per $km^2 - year$. Thus accurate measurement of UHECR is very difficult. Different detection strategies are implemented. When a UHECR particle enters into the atmosphere, serial interactions with atoms in the air are induced . This is called the air shower. The development of cosmic ray air shower is shown in Figure 1.2. We can catch UHCERs through measurements of air showers. Fluorescence detectors observe fluorescence light when atoms in the air are hit by air shower charge particles and cherenkov surface detetors made of scintillator arrays on the ground observe signals when air shower charge particles go through the detectors. Figure 1.3 depicts both detectors. The direction, energy and composition of the primory particle can be better determined by fluorescence detectors, but the duty time is limited to moonless nights. Thus surface detectors

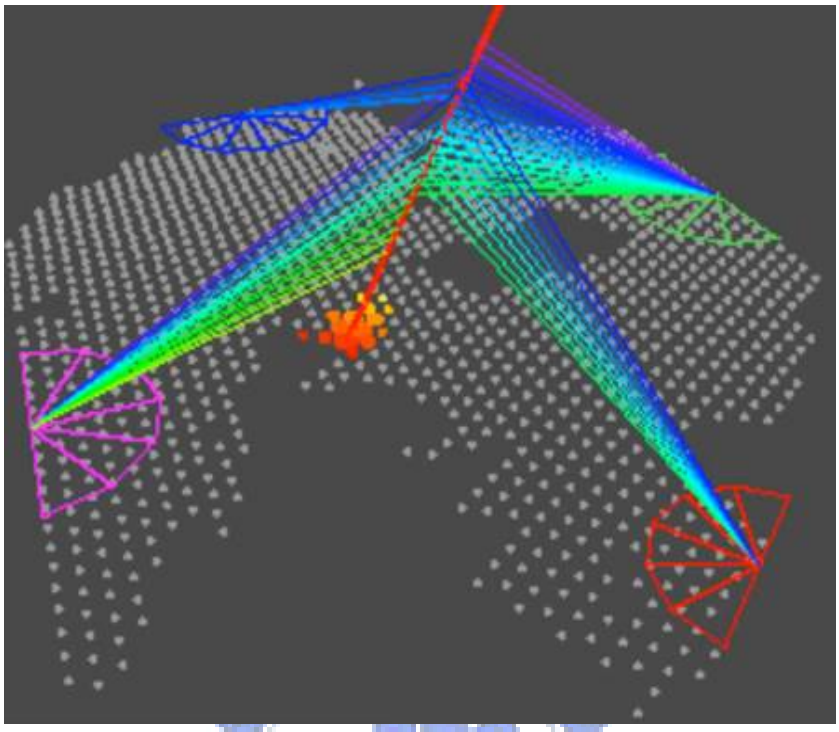

Figure 1.3: The fluorescence and surface detectors. This figure is taken from www.auger.org.

have more efficient exposure time. Figure 1.4 shows the map labelling the sites of four recent UHECR obervatories, where AGASA is a surface detector array, HiRes and Yakutsk are fluorescence detetors, and Auger is a hybrid detector. Auger has a surface detector array and four fluorescence detectors. They detect more events by the surface detectors and use the hybrid events detected by both kinds of detectors to perform the energy calibration.

1.2 Composition measurements

The composition of UHECRs can be determined by measuring the position of air shower maximum $X_{\max}$ through fluorescence detectors. Heavy nuclei have shorter $X_{\max}$ since the cross-sections of hadronic interaction increase with the amounts

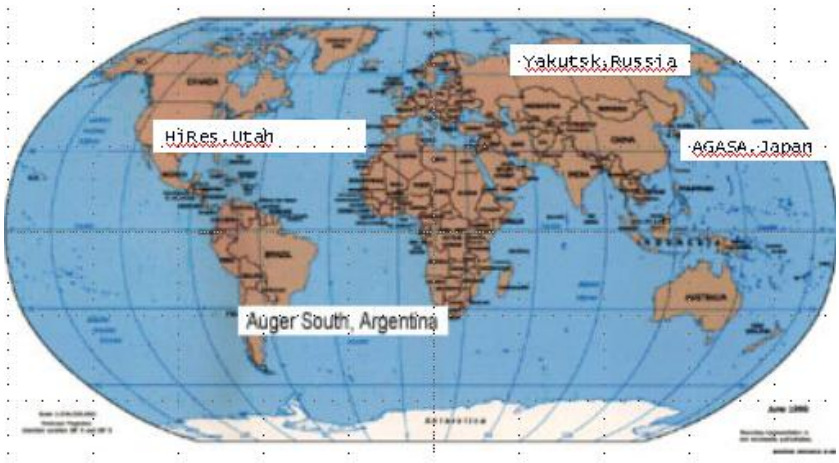

Figure 1.4: The Map labelling the sites of four recent UHECR observatories: AGASA in Japen, HiRes in US, Yakutsk in Russia, and Auger South in Argentina. This figure is taken from www.auger.org.

of nucleon. Figure 1.5 shows simulation results and measurements of several experiments. The data with energies above 4×10^{19} eV are still not availvable due to the short duty cycle of fluorescence detectors. However, the HiRes data seem to indicate a proton-dominated composition at the highest energy region while Auger's data favor heavy nuclei.

1.3 Features of UHECR spectra

The UHECR spectra measured from different observatories are presented in the left panel of Figure 1.6. Spectrum features are discussed as follows.

1.3.1 GZK cutoff

After cosmic microwave background was discovered in 1965, the Greisen-Zatsepin-Kuzmin cutoff was proposed in 1966 by Greisen [9],Zatsepin and Kuzmin [10]. They treated UHECR as protons, and considered their interactions with CMB photons during propagation. Among these interactions, the photo-pion production

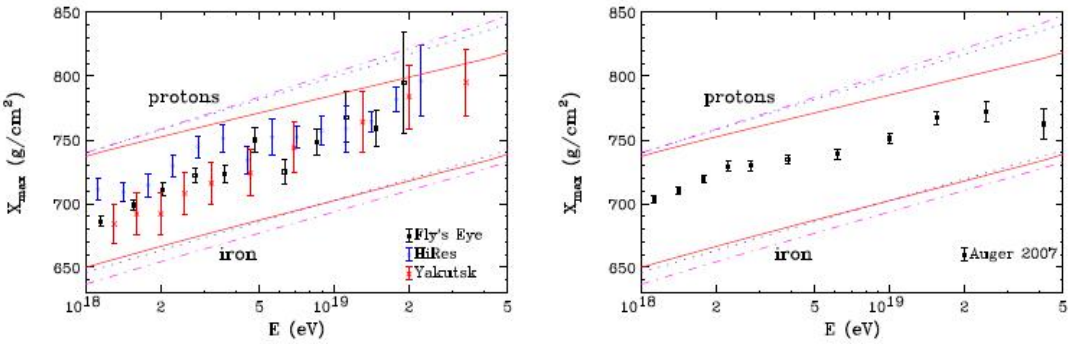

Figure 1.5: The values of $X_{\max}$ as a function of energy as measured by Fly's Eye, HiRes and Yakutsk (left panel) and as measured by Auger(right frame). The measurements are compared to the predictions for an all-proton and all-iron UHECR composition, using three different hadronic physics models. The magenta dot-dashed, red solid and blue dotted contours correspond to the models EPOS 1.6, QGSJET-III and SIBYLL 2.1, respectively. This figure is taken from[41].

$P\gamma \rightarrow P\pi$ is most efficient for proton energy loss. This inteaction reachs the maximum cross-section at the Δ-reasonace, where the invariant mass of photon and proton equals the Δ-mass. The corresponding proton energy is 5×10^{19} eV. Protons with energies greater than this value have an attenuation length of order 150 Mpc as showed in Figure 1.7. Thus the flux of protons with energies greater than 5×10^{19} eV is suppressed if their propagation distance is greater than 150 Mpc. This suppression is called GZK cutoff. The existence of GZK cutoff is worthy to be examined, because it offers the information about UHECR composition and origin. Fluxes exceeding GZK cutoff imply that these particles come from sources nearer than 150 Mpc. The GZK cutoff was confirmed by HiRes data[6] while disfavored by AGASA's[5]. This puzzle has not been resolved until Pierre Auger Observatory[7] confirms the findings of HiRes.

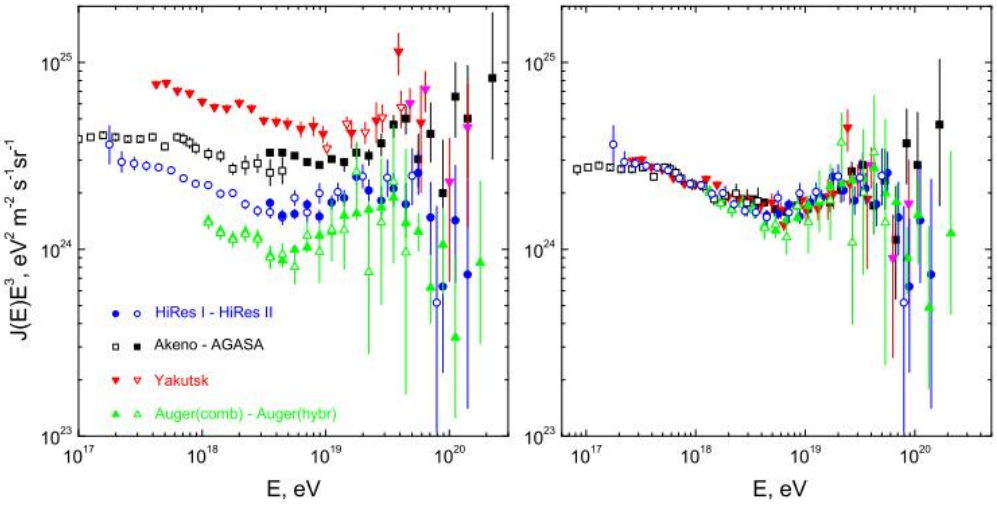

Figure 1.6: Left panel:UHECR spectra from different measurements. Right Panel: UHECR spectra after energy shift. This figure is taken from[11].

1.3.2 Energy calibration between different experiments

It is apparent that the fluxes obtained from different experiments are not consistent. The energy values corresponding to the dip and the GZK cutoff of UHECR spectrum were used to calibrate energy scales of different cosmic ray experiments [11, 12]. It has been shown that all measured UHECR energy spectra can be brought into good agreements by suitably adjusting the energy scale of each experiment [11]. We assume that HiRes energies are correct and the energies of all other detectors must be shifted by factor λ to reach the best agreement in fluxes. The energy-adjustment factor λ are found to be 1.2, 0.75, 0.83 and 0.625 for Auger, AGASA, Akeno and Yakutsk respectively. The resulted spectra are shown in the right panel of Figure 1.6. In addition, a different shower energy reconstruction method [13] gives rise to a 30% higher UHECR energy than that given by Auger's fluorescence detector-based shower reconstruction.

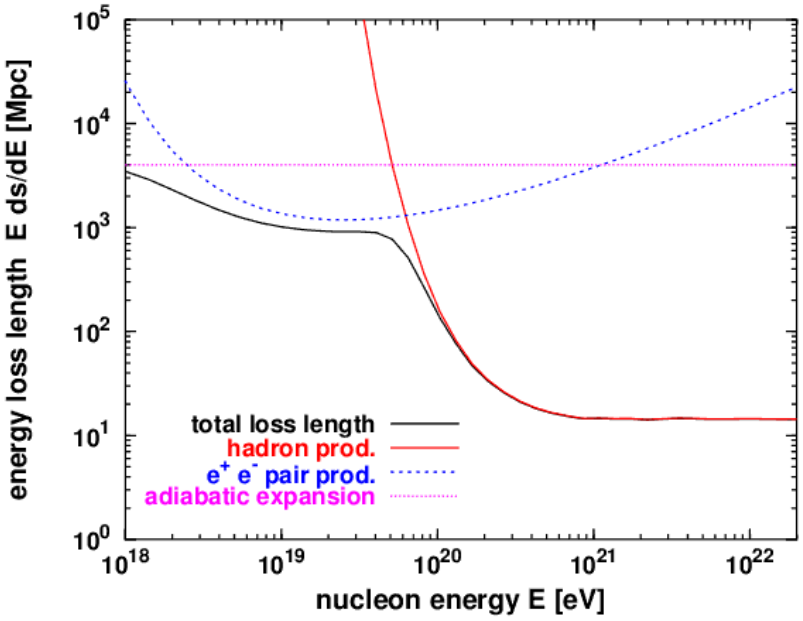

Figure 1.7: Attenuation lengths of cosmic rays energy loss processes: hadron production, pair production, and adiabatic expansion. Stanev et al. (2000).

1.4 Correlation sources search

Searching the accelerators is one of the most interesting topics of UHECRs. Several candidates based on the calculation of Fermi acceleration mechanism were proposed in Figure 1.8. Objects in active galaxies are proposed as sources of UHECRs. Recently, Pierre Auger observatory published results on correlation of the highest-energy cosmic rays with the positions of nearby active galactic nuclei (AGN) [1, 2]. Events and the correlated sources are marked in Figure 1.9. Such a correlation is confirmed by the data of Yakutsk [14] while it is not found in the analysis by HiRes [15]. In the Auger result, the correlation is maximal for the threshold energy of cosmic rays at 5.7×10^{19} eV, the maximal distance of AGN at 71 Mpc and the maximal angular separation of cosmic ray events at $\psi = 3.2°$. With the same threshold energy, and the angular separation $\psi \leq 6°$, the correlation remains strong for a range of maximal AGN distance between 50 Mpc and

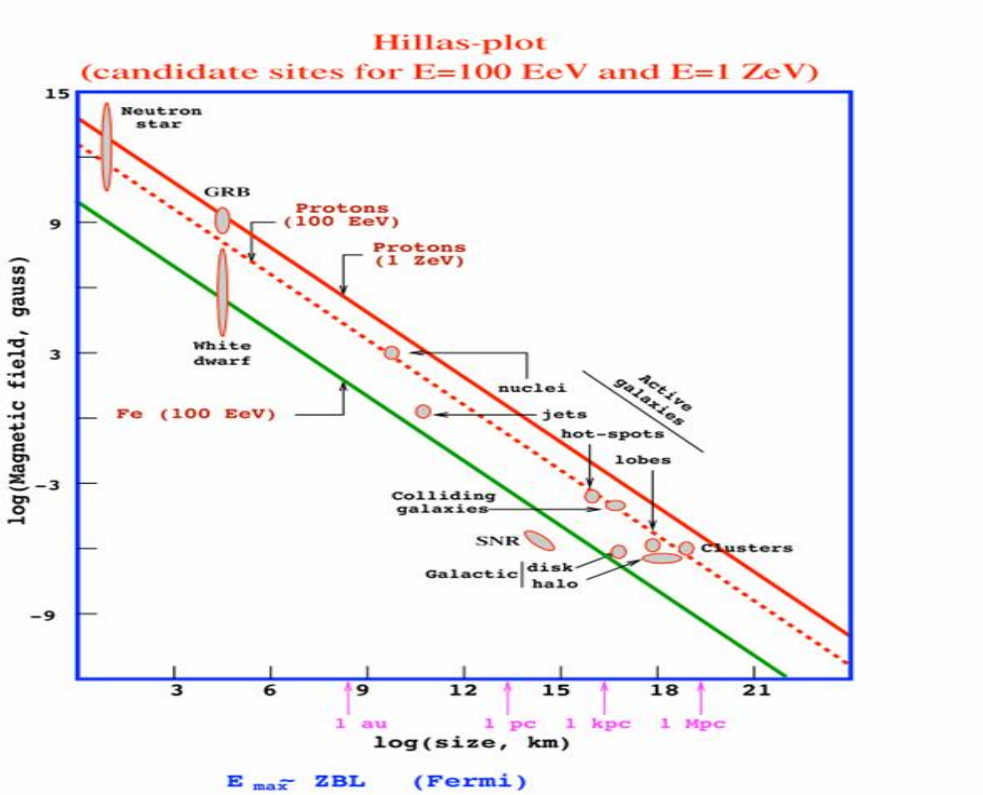

Figure 1.8: Candidates for UHECR sources in Hillas plot. A. M. Hillas. Ann. Rev. Astron. Astrophys., 22:425V444, 1984.

100 Mpc. Due to increasing efforts on verifying the Auger result, it is worthwhile to examine the above correlation from a phenomenological point of view.

1.5 GZK horizon and inconsistency in Auger's analysis

Since the angular scale of the observed correlation is only a few degrees, one expects that these cosmic ray particles are predominantly light nuclei. The effect of GZK attenuations on these cosmic ray particles [9, 10] can be described by a distance scale referred to as "GZK horizon" which is a function of the selected

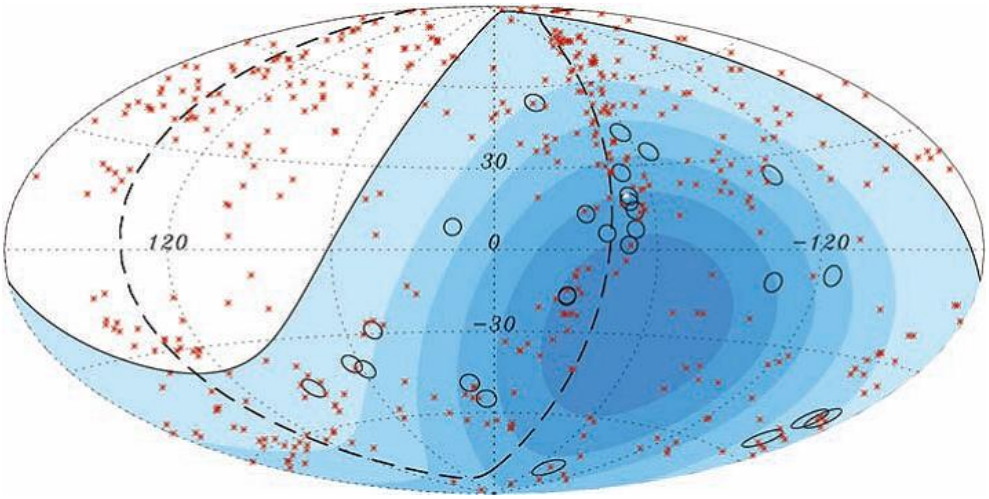

Figure 1.9: Aitoff projection of the celestial sphere in galactic coordinates with circles of radius 3.1° centered at the arrival directions of the 27 cosmic rays with highest energy detected by the Pierre Auger Observatory. The positions of the 472 AGN (318 in the field of view of the Observatory) with redshift $z \leq 0.018$ ($D < 75$ Mpc) from the 12^{th} edition of the catalog of quasars and active nuclei [19] are indicated by red asterisks. The solid line represents the border of the field of view (zenith angles smaller than 60°). Darker color indicates larger relative exposure. Each colored band has equal integrated exposure. The dashed line is the supergalactic plane. Centaurus A, one of our closest AGN, is marked in white. This figure is taken from[1].

energy threshold for the arriving cosmic ray particles. By definition, the GZK horizon associated with a threshold energy $E_{\rm th}$ is the radius of a spherical region which is centered at the Earth and produce 90% of UHECR events arriving on Earth with energies above $E_{\rm th}$. With continuous energy loss approximation, the GZK horizon for protons with $E_{\rm th} = 57$ EeV is about 200 Mpc by assuming a uniformly distributed UHECR sources with identical cosmic ray luminosity and spectral index [16]. The calculations based upon kinetic equation approach or stochastic energy loss also reach to similar conclusions [17, 18].

The departure of theoretically calculated GZK horizon to the maximum valid distance of the V-C catalog [19] employed in Pierre Auger's analysis, which is around 100 Mpc, can be attributed to several factors. As mentioned in [2], such a deviation may arise from non-uniformities of spatial distribution, intrinsic luminosity and spectral index of local AGN. In addition, the energy calibration also plays a crucial role since the GZK horizon is highly sensitive to the threshold energy $E_{\rm th}$.

1.6 Solutions to the departure between GZK horizon and valid distance of V-C catalog

As just stated, the V-C catalog used by Pierre Auger for the correlation study is complete only up to 100 Mpc while the GZK horizon for $E_{\rm th} = 57$ EeV is generally of the order 200 Mpc. In this thesis, we examine possible solutions to this departure,which are provided as follows.

1.6.1 Local over-density of UHECR sources

We first consider the local over-density of UHECR sources as a possible resolution to the above discrepancy. It is motivated by the existence of Local Supercluster (LS) which has a diameter of the order 60 Mpc. In LS, the over-density of galaxies has been estimated to be ~ 2 [20].

The local over-density of UHECR sources has been invoked [21, 22, 23] to account for AGASA data [4, 5]. Such a density distribution naturally leads to a smaller GZK horizon. However, it also significantly affects the UHECR energy spectrum in $(5 \cdot 10^{19} - 10^{20})$ eV region. Hence fittings to the measured UHECR spectrum [24] can provide information on the degree of local over-density. Subsequently, the magnitude of GZK horizon can be better estimated.

1.6.2 Effects of energy calibration

We next study the energy calibration effect on the estimation of GZK horizon and the spectrum of UHECR. Certainly a $20\% - 30\%$ upward shift on UHECR energies reduces the departure of theoretically calculated GZK horizon to the maximum valid distance of V-C catalog [2]. The further implications of this shift will be studied in fittings to the shifted Auger spectrum.

Chapter 2

Research methods

2.1 Cosmic ray propogation and energy loss

For single UHECR source, the cosmic-ray energy attenuation is governed by the equation

$$\frac{\partial \phi_N(E,t)}{\partial t} = \frac{\partial}{\partial E}\left[\left(-\frac{dE}{dt}\right)\phi_N(E,t)\right], \tag{2.1}$$

in the continuous energy loss approximation, where $\phi_N(E,t)$ is the flux of UHECR from the source. This equation results from the number conservation of cosmic-ray particles in the energy attenuation process. The cosmic-ray energy loss per unit time $-dE/dt$ is due to the cosmic expansion and its scattering with cosmic microwave background photons through photo-pion production process $P\gamma \to N\pi$ and pair production process $P\gamma \to Pe^+e^-$. The above attenuation equation is well known [25]. In the current context, the solution of Eq. (2.1) can be expressed in terms of the red-shift variable [23]

$$\phi_N(E,z) = \phi_N(\bar{E}, z_s) \times \exp\left[\int_z^{z_s} dz' \left(\frac{(1+z')}{H(z')} \times \frac{\partial b_0((1+z')\bar{E})}{\partial \bar{E}} + \frac{1}{1+z'}\right)\right], \tag{2.2}$$

where z_s is the red-shift of the UHECR source and the function b_0 is related to the rate of cosmic-ray energy loss at the present epoch by

$$-\frac{dE}{dt}(z=0) = b_0(E) + H_0 E, \tag{2.3}$$

where H_0 is the present value of Hubble constant. The UHECR has an energy $\bar{E}$ at the source with red-shift z_s and its energy is downgraded to E at the red-shift z. The energy $\bar{E}$ is a function of E and z so that $\bar{E}(E, z_s) = E$ and

$$\frac{d\bar{E}}{dz} = -\frac{b_0\left((1+z)\bar{E}\right)}{H(z)}(1+z) - \frac{\bar{E}}{1+z}. \tag{2.4}$$

Due to the non-trivial form of b_0, one resorts to numerical methods for computing the function $\bar{E}$ and the flux $\phi_N(E, z)$.

To discuss the UHECR spectrum at the highest energy, it is more appropriate to treat the cosmic ray energy loss as a stochastic process [27]. There are numerical packages available for treating stochastic energy loss of cosmic ray particles [28, 29]. We employ the latter package for our calculations. Although UHECR loses its energy mostly by scattering off CMB photons, it also loses some amount of energy by scattering off infrared background photons [30, 31, 32, 33, 34]. Thus we include the infrared photon contribution to the UHECR energy attenuation. We treat the energy attenuation by photo-pion production as a stochastic process while treating other attenuations as continuous processes.

2.2 Source evolution models

In the energy region we are interested, the source evolution at high redshifts $z > 1$ is not relevant. We simplify source evolution models as the form $n(z) = n_0(1+z)^m$, where m is an integer and n_0 is the source number density at the present epoch. The model $n(z) = n_0(1+z)^3$ is adopted in the calculation of GZK horizon and spectrum in this thesis. It is from the generally-accepted soft evolution model which traces the star formation history and has been adopted in previous works [35]. It also demonstrated that the effect on UHECR spectrum caused by varying m can be compensated by suitably adjusting the power index γ. A stronger evolution model with $m = 4.8$ was tested in [36]. The result is consistent with the conclusion in [35]. Varying m has no strong effect on the spectrum at highest energies, however, a stronger evolution model could give a larger neutrino flux. We do

not include this model in our calculation since this evolution is specialized for considering GRB as sources. To resolve the questions stated above, we further introduce a local over-density of sources. It is defined as

$$\begin{aligned} n(l < 30\text{Mpc})/n_0 &= k(1+z)^3, \\ n(l \geq 30\text{Mpc})/n_0 &= (1+z)^3. \end{aligned} \tag{2.5}$$

2.3 Spectrum fittings

We fit the UHECR spectrum for events with energies above 10^{19} eV. This is the energy range where the GZK attenuation exhibits its effect. It is also the energy range where the local over-density of UHECR sources shows significant effects. Spectrum fittings at this energy region offer information about degree of local over-density and GZK horizons. In our analysis, we take the UHECR as protons, which is hinted in the Auger events with energies $\geq$ 57 EeV although the composition study by the same group suggests a heavier composition for $E \leq 40$ EeV [37]. The HiRes experiment measures the composition up to 50 EeV [38] and obtains a composition lighter than that of Auger. For $E > 50$ EeV, the event number is still too small for the composition study.

Chapter 3

GZK horizons

3.1 The accumulative event probabilities of UHECR

To facilitate our discussions, we define the accumulative event probabilities of UHECR as

$$P(D, E_{\rm th}) = \frac{\int_0^D dl \cdot N(l, E_{\rm th})}{\int_0^\infty dl \cdot N(l, E_{\rm th})}, \tag{3.1}$$

where $N(l, E_{\rm th}) \cdot dl$ is the number of cosmic ray events which are originated from sources at distances between l and $l + dl$ from the Earth and arrive at the detector with energies above $E_{\rm th}$. We calculate $P(D, E_{\rm th})$ for various local over-densities of UHECR sources. The source distribution over the red-shift is taken as $n(z) = n_0(1+z)^3$ and the energy spectrum of each source is taken to be the form, $\phi_N(E) \equiv dN/dE = AE^{-\gamma}$, with the maximal energy $E_{\rm cut} = 1000$ EeV. We choose $\gamma = 2.4$, 2.5 and 2.6 where $\gamma = 2.5$ gives the best fitting to the measured UHECR spectrum as will be shown in the next section. The accumulative event probability $P(D, E_{\rm th})$ for $E_{\rm th} = 57$ EeV, 70 EeV, 80 EeV and 90 EeV are shown in Fig. 3.1 for $\gamma = 2.4$. Results for $\gamma = 2.5$ and $\gamma = 2.6$ are not distinguishable from those for $\gamma = 2.4$. In each panel, the red, green, blue, and black curves represent local over-density $n(l < 30{\rm Mpc})/n_0 = 1,\ 2,\ 4,$ and 10 respectively. The local over-density $n(l < 30{\rm Mpc})/n_0 = k$ is defined in Eq. (2.5). The horizontal dash line in each panel denotes $P(D, E_{\rm th}) = 0.9$. The intersection of this line with each color curve gives

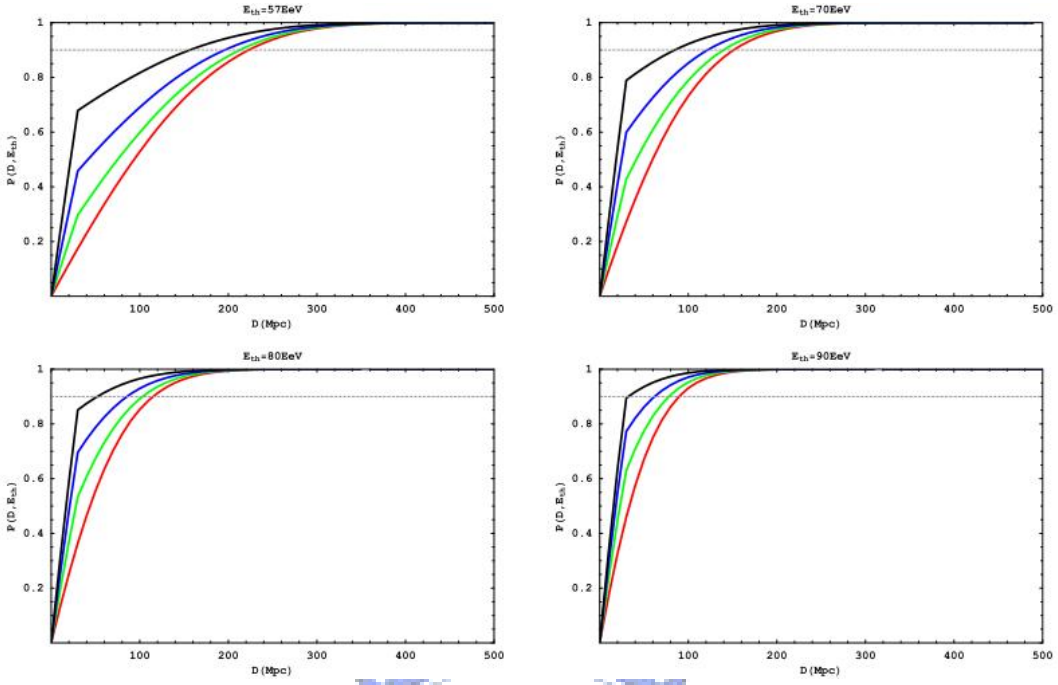

Figure 3.1: The accumulative event probability $P(D, E_{\rm th})$ as a function of D for $E_{\rm th}$ = 57 EeV, 70 EeV, 80 EeV and 90 EeV respectively. The horizontal dash line in each panel denotes $P(D, E_{\rm th}) = 0.9$. The red, green, blue and black curves represent results from models with over-density $n(l < 30{\rm Mpc})/n_0 = 1,\ 2,\ 4$, and 10 respectively. The intrinsic spectrum index $\gamma = 2.4$, energy cut $E_{\rm cut} = 1000$ EeV and the source evolution model $n(z) = n_0(1+z)^3$ are used for calculations.

the GZK horizon corresponding to a specific local over-density characterized by the ratio $n(l < 30{\rm Mpc})/n_0$.

3.2 GZK horizons and local over-densities

GZK horizons corresponding to different local over-densities and $E_{\rm th}$ are summarized in Table I. It is seen that local over-densities up to $n(l < 30{\rm Mpc})/n_0 = 4$ do not alter GZK horizons significantly for a given $E_{\rm th}$. One could consider possibilities for higher local over-densities. However, there are no evidences for such

Table 3.1: GZK horizons of UHECR calculated with the local over-density $n(l < 30\text{Mpc})/n_0 = 1,\ 2,\ 4$, and 10, and arrival threshold energy $E_{\text{th}} = 57$ EeV, 70 EeV, 80 EeV and 90 EeV respectively. The listed numbers are in units of Mpc.

$n(l < 30\text{Mpc})/n_0$	$E_{\text{th}} = 57\,\text{EeV}$	$E_{\text{th}} = 70\,\text{EeV}$	$E_{\text{th}} = 80\,\text{EeV}$	$E_{\text{th}} = 90\,\text{EeV}$
1	220	150	115	90
2	210	140	105	75
4	195	120	85	60
10	155	85	50	30

over-densities either from astronomical observations [20] or from fittings to the measured UHECR spectrum. We note that GZK horizons are rather sensitive to E_{th}. Table I shows that GZK horizons are ~ 100 Mpc or less for $E_{\text{th}} \geq 80$ EeV.

Chapter 4

Fittings to the UHECR spectrum measured by Pierre Auger

As mentioned earlier, the local over-density of UHECR sources affects the cosmic-ray spectrum at the highest energy, especially at energies higher than $5 \cdot 10^{19}$ eV. Hence the degree of local over-density can be examined through fittings to the measured UHECR spectrum as will be shown momentarily.

Fittings to the Auger spectrum have been performed in [26, 39, 40, 41]. In our work, we take into account the over-density of UHECR sources in the distance scale $l \leq 30$ Mpc. As stated previously, we take the UHECR to be protons.

4.1 Fittings to the unshifted spectrum

Figure 4.1 shows our fittings to the Auger measured UHECR spectrum with $\gamma = 2.5$ and 2.6. Figure 4.2 shows the case of $\gamma = 2.7$. We take the red-shift dependence of the source density as $n(z) = n_0(1+z)^m$ with $m = 3$. We have fitted 12 Auger data points beginning at the energy 10^{19} eV. We make a flux normalization at 10^{19} eV while varying the power index γ and the the degree of local over-density, $n(l < 30\text{Mpc})/n_0$. Part of χ^2 values from our fittings are summarized in Table II. For $\gamma = 2.4$, all the cases are disfavored by the fitting. $n(l < 30\text{Mpc})/n_0 = 1$

Table 4.1: The values of total χ^2 from fittings to the Auger measured UHECR spectrum. Numbers in the parenthesis are χ^2 values from fittings to the 8 data points in the energy range $19.05 \leq \log_{10}(E/\text{eV}) \leq 19.75$. The last 4 data points record events with energy greater than 71 EeV.

$n(l < 30\text{Mpc})/n_0$	1	2	4	10
$\gamma = 2.5$	14.12(9.34)	14.61(9.93)	17.09(10.50)	28.09(13.93)
$\gamma = 2.6$	16.64(12.28)	15.56(11.90)	16.01(11.83)	20.76(11.67)
$\gamma = 2.7$	25.77(20.71)	23.33(19.69)	21.16(18.08)	20.91(15.33)

gives the χ^2 value of 19.92 and the other χ^2 values increase monotonicly with the degree of over-density. The cases of $\gamma = 2.7$ are intriguing. The χ^2 values seem to be monotonicly decreasing with the degree of local over-density. Figure 4.2 gives the explanation. Since the fittings for $\gamma = 2.7$ are far below the data points, high degrees of over-density counteract this departure. We found that $\gamma = 2.5$, $n(l < 30\text{Mpc})/n_0 = 1$ gives the smallest χ^2 value with $\chi^2/\text{d.o.f.} = 1.57$. For the same power index, the large local over-density $n(l < 30\text{Mpc})/n_0 = 10$ is ruled out at the significance level $\alpha = 0.001$. For $\gamma = 2.6$, $n(l < 30\text{Mpc})/n_0 = 10$ is ruled out at the significance level $\alpha = 0.02$.

We note that, for both $\gamma = 2.5$ and $\gamma = 2.6$, the GZK horizon with $n(l < 30\text{Mpc})/n_0 = 10$, $E_{\text{th}} = 57$ EeV, $m = 3$ and $E_{\text{cut}} = 1000$ EeV is about 155 Mpc. Since $n(l < 30\text{Mpc})/n_0 = 10$ is clearly disfavored by the spectrum fitting, one expects a GZK horizon significantly larger than 155 Mpc for $E_{\text{th}} = 57$ EeV.

4.2 Fittings to the shifted spectrum

We next perform fittings to the shifted Auger spectrum. The results are shown in Figure 4.3 and Figure 4.4 where the cosmic ray energy is shifted upward by 30%. Part of χ^2 values are summarized in Table III. The smallest χ^2 value occurs approximately at $\gamma = 2.4$, $n(l < 30\text{Mpc})/n_0 = 2$ with $\chi^2/\text{d.o.f} = 0.82$. For $\gamma = 2.5$,

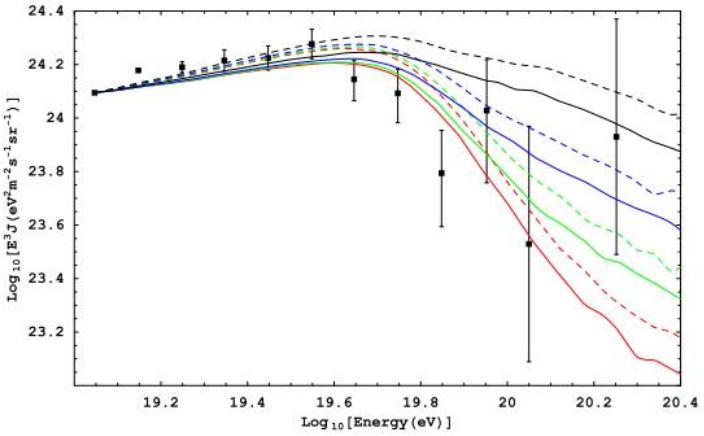

Figure 4.1: Fittings to the Auger measured UHECR spectrum where the red, green, blue and black curves denote the model with the local over-density $n(l < 30\text{Mpc})/n_0 = 1,\ 2,\ 4$, and 10 respectively. Solid curves correspond to $\gamma = 2.6$ while dash curves correspond to $\gamma = 2.5$. We take the source evolution parameter $m = 3$ throughout the calculations.

χ^2/d.o.f = 1.31, 0.96 and 0.87 for $n(l < 30\text{Mpc})/n_0 = 1$, 2 and 4 respectively. For $\gamma = 2.3$, $n(l < 30\text{Mpc})/n_0 = 1$, the χ^2 value is 12.89 and the others increase with the degree of local over-density monotonicly. For $\gamma = 2.6$, the behavior of the χ^2 values is the same with the one of $\gamma = 2.7$ for the unshifted spectrum. It is shown in Figure 4.4.

It is seen that χ^2 values from current fittings are considerably smaller than those from fittings to the unshifted spectrum. Given a significance level $\alpha = 0.1$, it is seen that every local over-density listed in Table III except for $\gamma = 2.4$ and 2.5, $n(l < 30\text{Mpc})/n_0 = 10$ is consistent with the measured UHECR spectrum. It is intriguing to test such local over-densities as will be discussed in the next section.

We note that, with a 30% upward shift of energies, the cosmic ray events analyzed in Auger's correlation study would have energies higher than 74 EeV

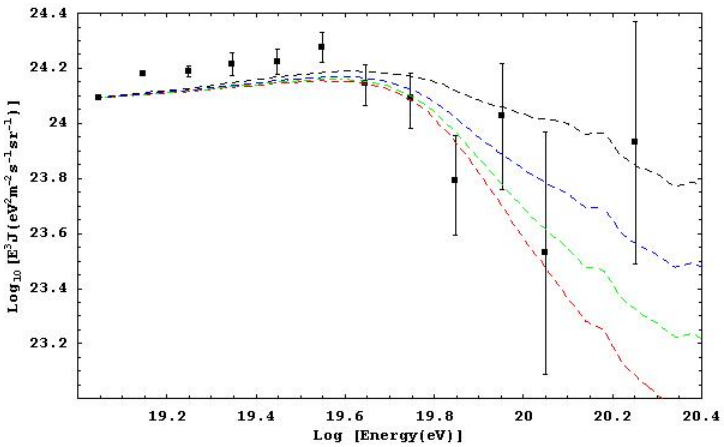

Figure 4.2: Fittings to the Auger measured UHECR spectrum where the red, green, blue and black curves denote the model with the local over-density $n(l < 30\text{Mpc})/n_0 = 1,\ 2,\ 4$, and 10 respectively. Here we take $\gamma = 2.7$ and the source evolution parameter $m = 3$ throughout the calculations.

instead of 57 EeV. The GZK horizon corresponding to $E_{\text{th}} = 74$ EeV is 120 Mpc for $n(l < 30\text{Mpc})/n_0 = 2$ and 105 Mpc for $n(l < 30\text{Mpc})/n_0 = 4$.

We have so far confined our discussions at $m = 3$. In the literature, m has been taken as any number between 0 and 5. It is demonstrated that the effect on UHECR spectrum caused by varying m can be compensated by suitably adjusting the power index γ [35]. Since GZK horizons are not sensitive to γ and m, results from the above analysis also hold for other m's.

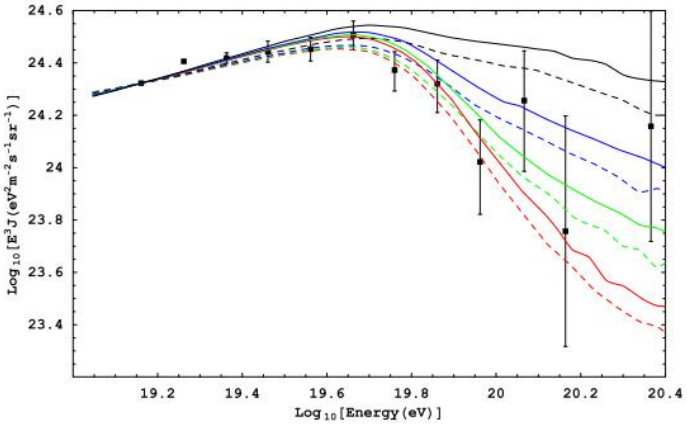

Figure 4.3: Fittings to the Auger measured UHECR spectrum with a 30% upward shift on UHECR energies where the red, green, blue and black curves denote the model with the local over-density $n(l < 30\text{Mpc})/n_0 = 1,\ 2,\ 4$, and 10 respectively. Solid curves correspond to $\gamma = 2.4$ while dash curves correspond to $\gamma = 2.5$. We take the source evolution parameter $m = 3$ throughout the calculations.

Table 4.2: The total χ^2 values from fittings to the Auger measured UHECR spectrum with a 30% upward shift on UHECR energies. Numbers in the parenthesis are χ^2 values from fittings to the 8 data points in the energy range $19.16 \leq \log_{10}(E/\text{eV}) \leq 19.86$. The last 4 data points record events with energy greater than 92 EeV.

$n(l < 30\text{Mpc})/n_0$	1	2	4	10
$\gamma = 2.4$	8.65(4.30)	7.39(4.67)	10.26(6.35)	27.31(13.34)
$\gamma = 2.5$	11.82(6.16)	8.67(5.49)	7.78(5.23)	16.18(7.39)
$\gamma = 2.6$	20.76(13.93)	16.08(11.84)	12.47(10.14)	13.91(8.64)

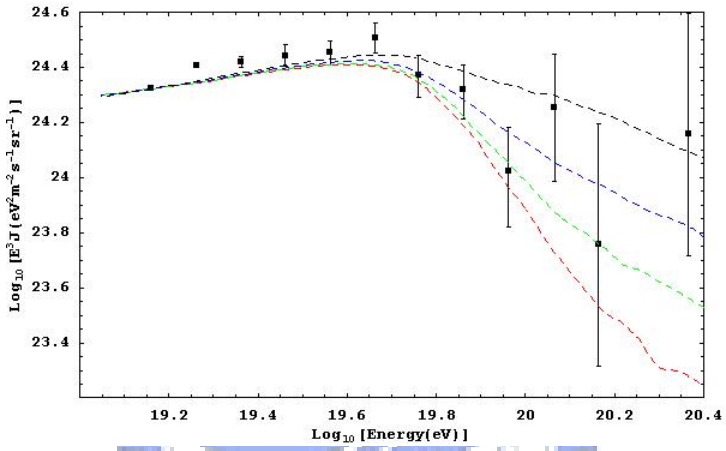

Figure 4.4: Fittings to the Auger measured UHECR spectrum with a 30% upward shift on UHECR energies where the red, green, blue and black curves denote the model with the local over-density $n(l < 30\text{Mpc})/n_0 = 1,\ 2,\ 4$, and 10 respectively. Here we take $\gamma = 2.6$ and the source evolution parameter $m = 3$ throughout the calculations.

Chapter 5

Conclusions

We have investigated the consistency between Auger's latest result on the correlation of UHECR sources with positions of nearby extra-galactic AGN and its measured UHECR spectrum. As stated before, this investigation is motivated by the fact that the V-C catalog used by Pierre Auger for the correlation study is reliable only up to 100 Mpc while the GZK horizon for $E_{\rm th} = 57$ EeV is generally of the order 200 Mpc. We have explored the possibility for local over-density of UHECR sources, which is expected to shorten the GZK horizon for a given threshold energy of arrival cosmic-ray particles. This is indeed the case as can be seen from Table I. On the other hand, the effect is far from sufficient to shorten the GZK horizon at $E_{\rm th} = 57$ EeV to ~ 100 Mpc for a local over-density of UHECR sources consistent with the measured UHECR spectrum.

We have performed a upward energy shift to the Auger measured UHECR spectrum. As said, a upward energy shift is motivated by simulations of shower energy reconstructions as well as the requirement of reproducing the theoretically predicted GZK cutoff energy. With a 30% energy shift, each cosmic ray event used by Auger for the correlation study would have an energy above 74 EeV instead of 57 EeV. GZK horizons corresponding to $E_{\rm th} = 74$ EeV then match well with the maximum valid distance of V-C catalog. Fittings to the shifted Auger spectrum indicate a possibility for the local over-density of UHECR sources.

We point out that the local over-density of UHECR sources is testable in the future cosmic ray astronomy where directions and distances of UHECR sources can be determined. Table IV shows percentages of cosmic ray events that come from sources within 30 Mpc for different values of $E_{\rm th}$ and $n(l < 30{\rm Mpc})/n_0$. We take $\gamma = 2.4$, $m = 3$ and $E_{\rm cut} = 1000$ EeV for calculating these percentages. We note that these percentages are not sensitive to the above parameters. For $E_{\rm th} = 57$

Table 5.1: Percentages of cosmic ray events that come from sources within 30 Mpc for different values of $E_{\rm th}$ and local over-density $n(l < 30{\rm Mpc})/n_0$.

$n(l < 30{\rm Mpc})/n_0$	$E_{\rm th} = 57\,{\rm EeV}$	$E_{\rm th} = 70\,{\rm EeV}$	$E_{\rm th} = 80\,{\rm EeV}$	$E_{\rm th} = 90\,{\rm EeV}$
1	0.17	0.27	0.36	0.46
2	0.30	0.43	0.53	0.63
4	0.46	0.60	0.70	0.77
10	0.68	0.79	0.85	0.89

EeV, only 17% of cosmic ray events come from sources less than 30 Mpc away for $n(l < 30{\rm Mpc})/n_0 = 1$. For $n(l < 30{\rm Mpc})/n_0 = 2$ and the same threshold energy, 30% of cosmic ray events are originated from sources in the same region.

It should be stressed that we have focused only on resolving the apparent discrepancy between the GZK horizon at $E_{\rm th} = 57$ EeV and the maximum valid distance of V-C catalog. The statistics analysis for establishing the source correlation is an independent issue beyond the scope of the current paper. We have found that the above discrepancy can not be resolved by merely introducing the local over-density of UHECR sources. On the other hand, if Auger's energy calibration indeed underestimates the UHECR energy, such a discrepancy can be reduced. More importantly, fittings to the shifted Auger spectrum indicate a possible local over-density of UHECR sources, which is testable in the future cosmic ray astronomy.

Bibliography

[1] J. Abraham *et al.* [Pierre Auger Collaboration], Science **318** (2007) 939 [arXiv:0711.2256 [astro-ph]].

[2] J. Abraham *et al.* [Pierre Auger Collaboration], Astropart. Phys. **29** (2008) 188 [arXiv:0712.2843 [astro-ph]].

[3] V. P. Egorova *et al.*, Nucl. Phys. Proc. Suppl. **136**, 3 (2004) [arXiv:astro-ph/0408493].

[4] N. Hayashida *et al.*, Phys. Rev. Lett. **73**, 3491 (1994).

[5] K. Shinozaki and M. Teshima [AGASA Collaboration], Nucl. Phys. Proc. Suppl. **136** (2004) 18.

[6] R. Abbasi *et al.* [HiRes Collaboration], Phys. Rev. Lett. **100**, 101101 (2008) [arXiv:astro-ph/0703099].

[7] P. Sommers [Pierre Auger Collaboration], arXiv:astro-ph/0507150.

[8] A. V. Olinto, AIP Conf. Proc. **745**, 48 (2005) [arXiv:astro-ph/0410685].

[9] K. Greisen, Phys. Rev. Lett. **16** (1966) 748.

[10] G. T. Zatepin and V. A. Kuz'min, Sov. Phys. JETP. Lett. **4** (1966) 78.

[11] V. Berezinsky, arXiv:0801.3028 [astro-ph].

[12] K. H. Kampert, arXiv:0801.1986 [astro-ph].

[13] R. Engel for the Pierre Auger Collaboration, arXiv:0706.1921 [astro-ph].

[14] A. A. Ivanov and f. t. Y. group, arXiv:0803.0612 [astro-ph].

[15] R. U. Abbasi *et al.*, arXiv:0804.0382 [astro-ph].

[16] D. Harari, S. Mollerach and E. Roulet, JCAP **0611** (2006) 012 [arXiv:astro-ph/0609294].

[17] O. E. Kalashev, B. A. Khrenov, P. Klimov, S. Sharakin and S. V. Troitsky, arXiv:0710.1382 [astro-ph].

[18] M. Kachelriess, E. Parizot and D. V. Semikoz, arXiv:0711.3635 [astro-ph].

[19] M.-P. Véron-Cetty and P. Véron, Astron. & Astrophys. **455** (2006) 773.

[20] P. J. E. Peebles, Principles of Physicsl Cosmology, Princeton University press, 1993; T. Stanev, R. Engel, A. Mucke, R. J. Protheroe and J. P. Rachen, Phys. Rev. D **62** (2000) 093005 [arXiv:astro-ph/0003484].

[21] M. Blanton, P. Blasi and A. V. Olinto, Astropart. Phys. **15** (2001) 275 [arXiv:astro-ph/0009466].

[22] V. Berezinsky, A. Z. Gazizov and S. I. Grigorieva, arXiv:hep-ph/0107306.

[23] V. Berezinsky, A. Z. Gazizov and S. I. Grigorieva, Phys. Rev. D **74** (2006) 043005 [arXiv:hep-ph/0204357].

[24] M. Roth [Pierre Auger Collaboration], arXiv:0706.2096 [astro-ph]; L. Perrone [Pierre Auger Collaboration], arXiv:0706.2643 [astro-ph]; P. Facal San Luis [Pierre Auger Collaboration], arXiv:0706.4322 [astro-ph].

[25] E. Lifshitz and L. Pitaevskii, Physical Kinetics: Landau and Lifschitz (Course of Theoretical Physics, Vol. **10** (Pergamon Press, Oxford, 1981)).

[26] V. Berezinsky, arXiv:astro-ph/0509069.

[27] T. Stanev, R. Engel, A. Mucke, R. J. Protheroe and J. P. Rachen, Phys. Rev. D **62** (2000) 093005 [arXiv:astro-ph/0003484].

[28] A. Mucke, R. Engel, J. P. Rachen, R. J. Protheroe and T. Stanev, Comput. Phys. Commun. **124** (2000) 290 [arXiv:astro-ph/9903478].

[29] E. Armengaud, G. Sigl, T. Beau and F. Miniati, Astropart. Phys. **28** (2007) 463 [arXiv:astro-ph/0603675].

[30] F. W. Stecker and M. H. Salamon, Astrophys. J. **512** (1999) 521 [arXiv:astro-ph/9808110].

[31] A. Franceschini, H. Aussel, C. J. Cesarsky, D. Elbaz and D. Fadda, arXiv:astro-ph/0108292.

[32] J. R. Primack, J. S. Bullock and R. S. Somerville, AIP Conf. Proc. **745** (2005) 23 [arXiv:astro-ph/0502177].

[33] G. Lagache, J. L. Puget and H. Dole, Ann. Rev. Astron. Astrophys. **43** (2005) 727 [arXiv:astro-ph/0507298].

[34] F. W. Stecker, M. A. Malkan and S. T. Scully, Astrophys. J. **648** (2006) 774 [arXiv:astro-ph/0510449].

[35] See, for example, D. De Marco and T. Stanev, Phys. Rev. D **72** (2005) 081301 [arXiv:astro-ph/0506318].

[36] H. Yuksel and M. D. Kistler, Phys. Rev. D **75**, 083004 (2007) [arXiv:astro-ph/0610481].

[37] M. Unger [The Pierre Auger Collaboration], arXiv:0706.1495 [astro-ph].

[38] Y. Fedorova et al. [HiRes Collaboration], *Proc. 30th ICRC, Mérida, Mexico* (2007) p. 1236.

[39] R. Aloisio, V. Berezinsky, P. Blasi, A. Gazizov, S. Grigorieva and B. Hnatyk, Astropart. Phys. **27** (2007) 76 [arXiv:astro-ph/0608219].

[40] K. Arisaka, G. B. Gelmini, M. Healy, O. Kalashev and J. Lee, JCAP **0712** (2007) 002 [arXiv:0709.3390 [astro-ph]].

[41] L. A. Anchordoqui, H. Goldberg, D. Hooper, S. Sarkar and A. M. Taylor, Phys. Rev. D **76** (2007) 123008 [arXiv:0709.0734 [astro-ph]].